Prepared for submission to JCAP

Constraining primordial vector mode from B-mode polarization

Shohei Saga,[a] **Maresuke Shiraishi,**[b,c] **Kiyotomo Ichiki**[a,d]

[a]Department of Physics and Astrophysics,
Nagoya University, Aichi 464-8602, Japan
[b]Dipartimento di Fisica e Astronomia "G. Galilei",
Università degli Studi di Padova, via Marzolo 8, I-35131, Padova, Italy
[c]INFN, Sezione di Padova,
via Marzolo 8, I-35131, Padova, Italy
[d]Kobayashi-Maskawa Institute for the Origin of Particles and the Universe,
Nagoya University, Nagoya 464-8602, Japan

E-mail: saga.shohei@nagoya-u.jp, maresuke.shiraishi@pd.infn.it,
ichiki@a.phys.nagoya-u.ac.jp

Abstract. The B-mode polarization spectrum of the Cosmic Microwave Background (CMB) may be the smoking gun of not only the primordial tensor mode but also of the primordial vector mode. If there exist nonzero vector-mode metric perturbations in the early Universe, they are known to be supported by anisotropic stress fluctuations of free-streaming particles such as neutrinos, and to create characteristic signatures on both the CMB temperature, E-mode, and B-mode polarization anisotropies. We place constraints on the properties of the primordial vector mode characterized by the vector-to-scalar ratio r_v and the spectral index n_v of the vector-shear power spectrum, from the *Planck* and BICEP2 B-mode data. We find that, for scale-invariant initial spectra, the ΛCDM model including the vector mode fits the data better than the model including the tensor mode. The difference in χ^2 between the vector and tensor models is $\Delta\chi^2 = 3.294$, because, on large scales the vector mode generates smaller temperature fluctuations than the tensor mode, which is preferred for the data. In contrast, the tensor mode can fit the data set equally well if we allow a significantly blue-tilted spectrum. We find that the best-fitting tensor mode has a large blue tilt and leads to an indistinct reionization bump on larger angular scales. The slightly red-tilted vector mode supported by the current data set can also create $\mathcal{O}(10^{-22})$-Gauss magnetic fields at cosmological recombination. Our constraints should motivate research that considers models of the early Universe that involve the vector mode.

arXiv:1405.4810v2 [astro-ph.CO] 11 Sep 2014

Contents

1 Introduction **1**

2 Vector mode induced by free-streaming particles **2**

3 Constraints on the primordial vector mode **4**
- 3.1 One-parameter estimate for scale-invariant cases 4
- 3.2 Two-parameter estimate 5
- 3.3 Constraints on r_v, n_v, and r_t 6

4 Conclusion **7**

1 Introduction

The Cosmic Microwave Background (CMB) radiation is an essential probe for verifying the standard cosmology and inflation models. The linear perturbations in the standard cosmology can be decomposed into the scalar mode (the curvature perturbation or the density perturbation) and the tensor mode (the primordial gravitational wave). Within these decompositions, the vector mode (i.e., the vorticity) is usually ignored since the vector mode only allows decaying solutions in the absence of sources. However, there are many models containing non-decaying solutions in the vector-mode sector (e.g., refs. [1–3]).

The scalar mode is known to generate CMB temperature and E-mode polarization fluctuations. CMB observations by satellites, such as COBE [4], WMAP [5], and *Planck* [6, 7] are consistent with theoretical predictions associated with the scalar-mode sector. These precise observations also determine the standard cosmological parameters and give us rich information about our Universe.

In addition to the temperature and E-mode fluctuations, the vector and tensor modes can also induce B-mode fluctuations [8–10]. Recently, the BICEP2 experiment detected the B-mode polarization with a tensor-to-scalar ratio normalized by $k = 0.05\mathrm{Mpc}^{-1}$, $r_{0.05} = 0.2^{+0.07}_{-0.05}$. In other words, $r_{0.05} = 0$ is disfavored at 7σ [11]. The result may be attributed straightforwardly to the detection of primordial gravitational waves, which are well studied since they provide direct information on inflation in the early universe [12–14]. The primordial gravitational waves may explain the B-mode polarization spectrum of the BICEP2 results for $\ell \lesssim 150$. However, some debate exists over the BICEP2 result. The tensor-to-scalar ratio based on the BICEP2 B-mode data is somewhat larger than the limit from the *Planck* temperature data. Some works explain this discrepancy by introducing the anti-correlated temperature spectrum [15–17]. In addition, another issue discussed in the literature is on the excess of the B-mode polarization spectrum at $150 \lesssim \ell \lesssim 250$ [18, 19]. These studies suggest the existence of something else, such as the vector mode. After the release of the BICEP2 results, some works discuss the constraints on the vector mode induced by magnetic fields [20], cosmic defects [18, 19] and self-ordering scalar fields [21].

Another solution to this discrepancy is foreground emission from the Galaxy. Indeed, it is pointed out that the level of the foreground contamination in the B-mode power spectrum presented in the BICEP2 paper may be underestimated [22], and the galactic, polarized dust emission should contribute to some extent to the BICEP2 B-mode signal. In ref. [22] it

is shown that the foreground dust can mimic the polarization signal of the BICEP2 power spectrum and can relax the above-mentioned tension between the temperature and polarization anisotropies. However, at the moment we have no reliable template for the foreground polarization emissions and must wait for the *Planck* polarization result, which is expected to be available later this year.

The purpose of the present paper is to update the constraints in Ref. [23] including the B-mode polarizations and to investigate the role of B-mode polarizations in constraining the primordial tensor and vector modes. Although there are many scenarios including the vector mode, in the present paper, we focus in particular on the vector mode sustained by the anisotropic stress fluctuations of free-streaming particles such as neutrinos [23–25]. In the standard cosmology with perfect fluids, the vector mode contains only a decaying mode. However, the anisotropic stress fluctuations of free-streaming particles can lead to the non-decaying vector mode. It is known that this vector mode induces additional B-mode fluctuations and behaves quite differently from the primordial tensor mode. The initial conditions of such a vector mode are characterized by two parameters associated with the vector-mode shear: the vector-to-scalar ratio r_v and the spectral index n_v of the power spectrum. In the present paper, we show constraints on these parameters with the other relevant parameters from both the BICEP2 B-mode and *Planck* temperature data.

This paper is organized as follows. In the next section, we briefly summarize the vector mode sustained by the anisotropic stress fluctuations of free-streaming particles and present the parameterization for the vector mode. In section 3, we obtain constraints on the vector mode together with the other relevant parameters. The final section is devoted to the conclusion of the paper.

2 Vector mode induced by free-streaming particles

In this section, we review the vector mode induced by free-streaming particles [23, 25]. The metric is given by

$$ds^2 = a^2 \left[-d\eta^2 + (\delta_{ij} + h_{ij})\, dx^i dx^j \right] \ , \tag{2.1}$$

where η is the conformal time and h_{ij} is the metric perturbation. In the standard cosmological perturbation theory, the scalar, vector, and tensor modes do not mix in the evolution equations. In this case, the metric perturbation of the vector mode can be written as

$$h_{ij}(\eta, \mathbf{x}) = \int \frac{d^3k}{(2\pi)^3} \sum_{\lambda=\pm1} h^{(\lambda)} \left[\hat{k}_i \epsilon_j^{(\lambda)}(\hat{k}) + \hat{k}_j \epsilon_i^{(\lambda)}(\hat{k}) \right] e^{i\mathbf{k}\cdot\mathbf{x}} \ , \tag{2.2}$$

where we have translated in Fourier space. Here $\epsilon_i^{(\lambda)}(\hat{k})$ is the divergenceless polarization vector and $\lambda = \pm 1$ indicates the helicity state of the vector mode. Note that $h^{(+1)}$ and $h^{(-1)}$ evolve independently from each other because the usual Einstein gravity contains the parity symmetry.

From here on, we omit the superscript λ for simplicity. The Einstein equations for the vector mode are [23, 25]

$$\dot{\sigma} + 2\mathcal{H}\sigma = -8\pi G a^2 p \Pi / k \ , \tag{2.3}$$

$$k^2 \sigma = 16\pi G a^2 q \ , \tag{2.4}$$

where we have defined the new variables, $\sigma \equiv \dot{h}/k$, $q \equiv (\rho + p)v$, and Π, which are the shear, the heat flux, and the anisotropic stress fluctuations for the vector mode, respectively. Here a

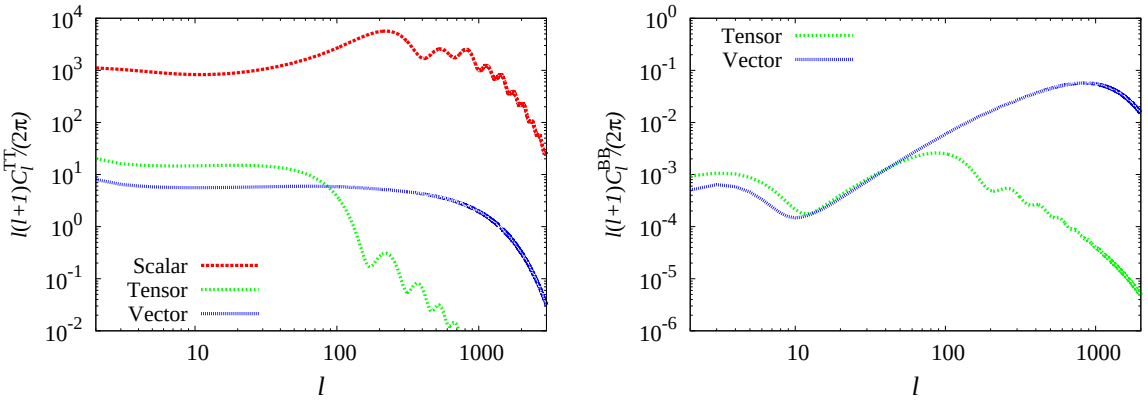

Figure 1. Power spectra of the CMB temperature (*left*) and B-mode (*right*) fluctuations induced from the scale-invariant vector ($n_v = 1$) and tensor ($n_t = 0$) power spectra. For the vector mode, we use the best-fitting amplitude $r_v = 4.3 \times 10^{-4}$ derived in section 3.3, while the tensor-to-scalar ratio r_t is adjusted to have the same B-mode amplitude at $50 \lesssim \ell \lesssim 100$ for comparison.

dot represents the derivative with respect to the conformal time. Note that if the anisotropic stress fluctuations are not the source of the shear, the metric perturbation of the vector mode contains only a decaying mode.

In the present analysis, we consider the standard cosmology with free-streaming particles, such as neutrinos. In this case, the vector shear σ is effectively supported by nonzero anisotropic stress fluctuations of neutrinos posterior to their decoupling ($T \sim 1$ MeV) via the above Einstein equations. These variables act as sources of the CMB anisotropies during the recombination epoch [23, 25].

In figure 1, we depict the CMB temperature fluctuation and B-mode polarization spectra for the scale-invariant cases, [i.e., $n_v = 1$ and $n_t = 0$ in eqs. (2.6) and (2.9)], in order to show the shape of the spectra. As shown in the figure, unlike for the tensor mode, the vector mode enhances small-scale temperature and polarization signals to the scale where the Silk damping is effective, namely $\ell \sim 1000$. More precisely, the temperature spectrum, C_ℓ^{TT} is mainly sourced by the baryon velocity in the Newtonian gauge, which is constant until the Silk damping effect occurs. At this point, the temperature spectrum becomes constant for $\ell \lesssim 1000$. However, the B-mode spectrum is sourced by the anisotropic stress fluctuations of photons and the E-mode polarization quadrupole.

Interestingly, because of these characteristics, if the vector and tensor B-mode spectra have almost the same amplitudes near $\ell = 100$, then the CMB temperature spectrum induced by the tensor mode is greater than that induced by the vector mode. This fact will yield a result that the vector mode is favored by the *Planck* and BICEP2 data in the scale-invariant case, which will be shown in section 3.1.

Considering the vector mode quantitatively, we parameterize the primordial vector spectrum as follows

$$\left\langle \sigma(\mathbf{k})\sigma^*(\mathbf{k}')\right\rangle \equiv (2\pi)^3 \frac{2\pi^2}{k^3}\mathcal{P}_v(k)\delta^{(3)}(\mathbf{k}-\mathbf{k}') \ , \tag{2.5}$$

$$\mathcal{P}_v \equiv \mathcal{A}_v \left(\frac{k}{k_{v0}}\right)^{n_v-1} \ , \tag{2.6}$$

where $\mathcal{A}_v$ is the amplitude of the primordial vector mode, n_v is the spectrum index of the

vector mode, $k_{v0} = 0.01$ Mpc^{-1} is the pivot scale of the vector mode, and the bracket means the ensemble average. Furthermore, we define the vector-to-scalar ratio as

$$r_v \equiv \frac{\mathcal{A}_v}{\mathcal{A}_s} \ , \tag{2.7}$$

where $\mathcal{A}_s$ is the primordial amplitude of the scalar mode. In terms of the power spectra of scalar and tensor modes, we follow the usual definitions:

$$\mathcal{P}_s(k) = \mathcal{A}_s \left(\frac{k}{k_{s0}}\right)^{n_s - 1 + \frac{1}{2}\alpha_s \ln(k/k_{s0})} \ , \tag{2.8}$$

$$\mathcal{P}_t(k) = \mathcal{A}_s r_t \left(\frac{k}{k_{t0}}\right)^{n_t} \ , \tag{2.9}$$

where r_t, n_s, n_t, and $\alpha_s \equiv dn_s/d\ln k$ are the usual tensor-to-scalar ratio, the scalar spectral index, the tensor spectral index, and the scalar running index, respectively. In the present paper, we choose the pivot scales of the scalar and tensor modes to be $k_{s0} = 0.05$ Mpc^{-1} and $k_{t0} = 0.01$ Mpc^{-1}, respectively.

3 Constraints on the primordial vector mode

In this section, we present constraints on the five parameters related to the vector and tensor modes and the scalar running index, i.e., r_v, n_v, r_t, n_t, and α_s, from the *Planck* temperature, WMAP E-mode (WP), and BICEP2 B-mode data, combined with a compilation of Baryon Acoustic Oscillation (BAO) data [26–28]. The observed CMB power spectra are expressed as the sum of the scalar, vector, and tensor spectra as $C_{\ell\ \rm tot}^{XX} = C_{\ell\ \rm scal}^{XX} + C_{\ell\ \rm vec}^{XX} + C_{\ell\ \rm tens}^{XX}$, where $X = T$ (temperature), E (E-mode polarization), and B (B-mode polarization), respectively. We ignore the TB and EB correlations since there is no parity violation in the standard cosmology discussed in the present paper. To estimate the constraints on the vector mode, we modify the latest public Monte-Carlo simulation code `CosmoMC` [29], in which the BICEP2 likelihood files have already been included.

In the following analysis, we vary r_v, n_v, r_t, n_t and α_s together with the default six parameters: the present baryon and CDM density parameters, the angular size of the sound horizon, the optical depth, and the amplitude and spectral index of the scalar power spectrum ($\Omega_b h^2$, $\Omega_c h^2$, $\theta_{\rm MC}$, τ, A_s, and n_s). The prior ranges are shown in Table 1.

Note that our prior ranges are chosen ad hoc, and not for a model selection through an evidence calculation. Instead, we focus on showing how the models fit the given data by comparing the likelihood or the effective chi-square values. To decide which model is favored by given data, one should account for the full prior range in the Bayesian evidence.

3.1 One-parameter estimate for scale-invariant cases

To begin with, let us estimate r_v and r_t, separately with the assumption that the vector or tensor power spectrum is scale invariant, i.e. $n_v = 1$ or $n_t = 0$. The resulting effective chi-squares are 8717.774 and 8721.068 respectively for r_v and r_t; the vector model provides a better fit to the *Planck* temperature and BICEP2 B-mode data set than does the tensor model. This result occurs because the amplitude of the temperature power spectrum on large scales induced by the vector mode is smaller than that by the tensor mode as shown in

Parameter	Prior range
$\Omega_b h^2$	$[0.005 : 0.1]$
$\Omega_c h^2$	$[0.001 : 0.99]$
$100\theta_{\rm MC}$	$[0.5 : 10]$
τ	$[0.01 : 0.8]$
$\ln(10^{10} A_s)$	$[2.7 : 4.0]$
n_s	$[0.9 : 1.1]$

Parameter	Prior range	Baseline
α_s	$[-0.5 : 0.5]$	0
r_v	$[0 : 0.2]$	0
n_v	$[-2.0 : 6.0]$	1
r_t	$[0 : 1.0]$	0
n_t	$[-2.0 : 5.0]$	0

Table 1. Prior ranges of six standard parameters (*left*) and five additional ones (*right*). The column "Baseline" gives the values used in the analysis when the corresponding parameter is fixed. Note that we do not use the consistency relation, $r_t = -8n_t$. In other words, the tensor spectral index n_t runs freely. The prior ranges for the vector mode parameters are matched to ref. [23]. The amplitudes of the CMB fluctuations induced by the vector mode are comparable to that by the tensor mode when $r_v/r_t \approx 10^{-2}$ [25]. Therefore we can set the vector-to-scalar ratio to be less than the tensor-to-scalar ratio.

(i) Vector mode		
parameters	best fit	68% limits
$10^4 r_v$	6.8	$6.2^{+1.14}_{-1.31}$
n_v	0.47	$0.55^{+0.194}_{-0.263}$
$\chi^2 = 8715.696$		$(\Delta\chi^2 = 2.593)$

(iii) Running index		
parameters	best fit	68% limits
r_t	0.17	$0.19^{+0.037}_{-0.046}$
α_s	-0.029	$-0.029^{+0.0074}_{-0.0074}$
$\chi^2 = 8714.250$		$(\Delta\chi^2 = 1.147)$

(ii) Tensor mode		
parameters	best fit	68% limits
r_t	0.16	$0.17^{+0.045}_{-0.051}$
n_t	2.0	$1.7^{+0.45}_{-0.40}$
$\chi^2 = 8713.103$		

(iv) Vector and Tensor modes		
parameters	best fit	68% limits
r_t	0.076	$0.069^{+0.032}_{-0.041}$
$10^4 r_v$	3.4	$4.1^{+1.3}_{-1.4}$
$\chi^2 = 8715.231$		$(\Delta\chi^2 = 2.128)$

Table 2. Best-fit values and 1σ (marginalized) limits on model parameters in analyses with vector mode alone (r_v, n_v) (*top left*), the tensor mode alone (r_t, n_t) (*bottom left*), the BICEP2 like parameterization $(r_t, \alpha_s, n_t = 0)$ (*top right*) and the vector and tensor modes with scale invariant spectra $(r_v, r_t, n_v = 1, n_t = 0)$ (*bottom right*). Here, $\Delta\chi^2$ in the brackets gives the differences of χ^2 from the value in the tensor mode alone parameterization. The results show that χ^2 for the tensor mode alone case is the smallest among the four cases.

figure 1 when the vector or tensor mode with the scale invariant spectra is fitted to the B-mode spectrum at the BICEP2 B-mode region, $50 \lesssim \ell \lesssim 300$. This result arises from the fact that, as we mentioned in the previous section, the vector mode creates the CMB fluctuations on small scales, while the tensor mode creates them on large scales. In other words, the vector mode can create the B-mode polarization with little effect on the temperature power spectrum compared with the tensor one.

3.2 Two-parameter estimate

We now constrain the four sets of the two model parameters: (i) (r_v, n_v), (ii) (r_t, n_t), (iii) (r_t, α_s) and (iv) (r_v, r_t). The results are shown in Table 2. We find that the (r_t, n_t) case can minimize the effective chi-square; namely, the tensor mode-only case with the relaxed

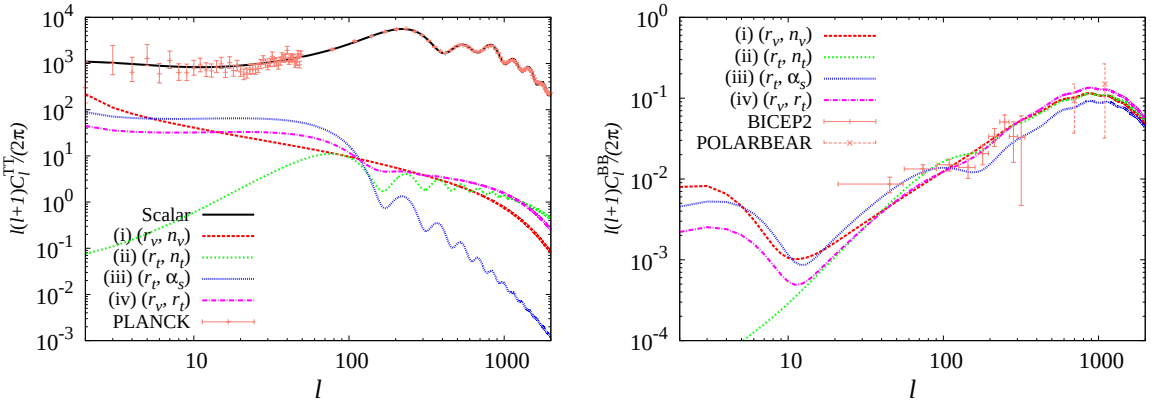

Figure 2. Power spectra of CMB temperature (*left*) and B-mode (*right*) fluctuations with best-fit parameters given in Table. 2. Note that the bump of the reionization epoch in the case of (r_t, n_t) becomes ambiguous since this parameterization leads to a very blue spectrum to suppress on large scales in the temperature spectrum [30–32]. For reference, the spectrum induced by the adiabatic scalar-mode is also shown in the left panel. We also show the B-mode spectrum detected by the POLARBEAR experiment [33]. We do not use the POLARBEAR data in our analysis as they are not as constraining as the other datasets considered.

inflationary-consistency relation fits the data better than the vector-mode cases (r_v, n_v) and (r_t, α_s) do.

The reasons for this result may come from analyzing figure 2, which shows the best-fit CMB temperature and B-mode power spectra. The right panel shows that the four curves are very nearly consistent with each other for $\ell > 10$ and all of them fit the BICEP2 B-mode data well. However, as seen in the left panel, the shape of each temperature spectrum is quite different. The case of (r_t, n_t) is consistent with the BICEP2 data when the tensor mode spectrum is blue-tilted, i.e., $n_t = 2.0$. In this case, the large-scale temperature signals are damped and are consistent with the *Planck* temperature data [30–32]. Furthermore, damping the large-scale B-mode signals makes the reionization bump ambiguous. However the other three cases are less suitable because of the large-scale temperature contributions. In particular, the temperature signals from the vector-mode case (r_v, n_v) are significant on very large scales because a slightly red-tilted spectrum ($n_v = 0.47$) is required to fit the BICEP2 B-mode data, making it most inconsistent.

3.3 Constraints on r_v, n_v, and r_t

In this subsection, we constrain the three additional parameters r_v, n_v, and r_t at the same time, as discussed in ref. [23]. In that paper, the authors used the observational data of the temperature and E-mode polarization given only by the WMAP experiment. We show here how the constraints are improved by the new temperature and B-mode data from *Planck* and BICEP2. Note that the running index of the initial scalar amplitude α_s is fixed to zero in this subsection.

Figure 3 depicts the marginalized two-dimensional posteriors for (r_v, n_v) and (r_v, r_t). Note that we assume $n_t = 0$, (i.e., the scale-invariant spectrum of the tensor mode), instead of the usual consistency relation $r_t = -8n_t$. The figure shows that the *Planck* temperature and BICEP2 B-mode data constrain r_t, r_v, and n_v strongly. From the *left* panel, we notice the interesting result that the BICEP2 data fits a smaller n_v whereas the other data without

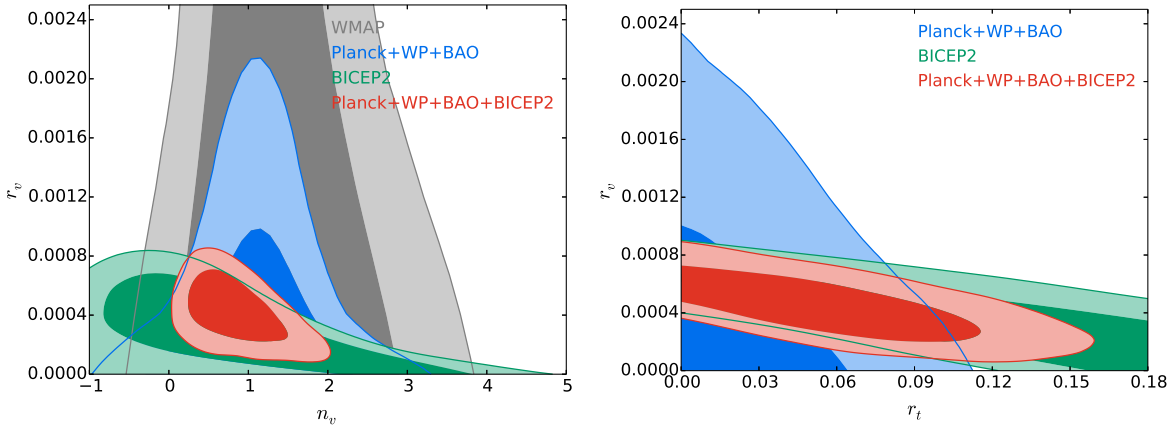

Figure 3. Marginalized two-dimensional posteriors for (r_v, n_v) (*left*) and (r_v, r_t) (*right*) obtained from *Planck*+WP (blue) and *Planck*+WP+BICEP2 (red). To compare with the previous study [23], in the *left* panel, we also describe the constraint from the WMAP temperature and polarization data (gray). For reference, we also show the marginalized two-dimensional posteriors obtained by the BICEP2 data alone (green) which are derived with the six standard cosmological parameters fixed to the *Planck* results as in Ref. [31].

the B-mode indicates a somewhat larger n_v. Concerning r_v and r_t, the *right* panel tells us that, by combining the BICEP2 result with the other data, a nonzero r_v is favored, while r_t is still consistent with null. Again, this is because the vector mode does not modify the temperature anisotropies as much as does the tensor mode for the nearly scale-invariant cases if the magnitude of the resulting B-mode spectrum is comparable to the BICEP2 data, as discussed in section 2. The marginalized limits for the *Planck*+WP+BAO+BICEP2 estimate are, given by $r_v = 4.3^{+1.6}_{-1.6} \times 10^{-4}$, $n_v = 0.83^{+0.28}_{-0.48}$, and $r_t < 0.09$.

In ref. [23], the authors also discuss the possibility that this vector mode creates seed magnetic fields that may be amplified through the dynamo mechanism to become the micro-Gauss-level magnetic fields associated with galaxies and clusters of galaxies (e.g. ref. [34]). The dynamo process needs the seed fields whose strength are as large as $10^{-20} \sim 10^{-30}$Gauss at the recombination epoch [35]. Theoretically, the vorticity driven by the vector shear produces rotational electric fields that can change to magnetic fields via the Maxwell constraint equation. The authors showed that $\mathcal{O}(10^{-21})$-Gauss magnetic fields at $k \approx 0.1$ Mpc^{-1}, which are required at the recombination epoch, can be produced by the r_v and n_v allowed by WMAP. Here, let us consider the generation of magnetic fields with the new parameter regions. When we adopt the above best-fit parameters, the amplitude of magnetic fields is about 10^{-22} Gauss at $k = 0.1$ Mpc^{-1} at cosmological recombination. This value is comparable to or slightly less than the result of ref. [23] but the amplitude may be large enough to be the seed magnetic fields.

4 Conclusion

If vector modes exist in the early Universe, and they evolve with the support of anisotropic stress fluctuations of free-streaming particles like neutrinos, they produce CMB temperature, E-mode, and B-mode anisotropies whose shapes are quite different from the scalar-mode and tensor-mode anisotropies typically considered. In the present paper, we investigate how such vector-mode signals are constrained from the latest temperature and B-mode data provided

by *Planck* and BICEP2 in comparison with the tensor mode. Next, by using a Monte-Carlo approach, we estimate observational bounds on the vector-to-scalar ratio, r_v, and the spectral index, n_v, associated with the primordial power spectrum of the vector-mode shear, combined with the usual scalar-mode and several tensor-mode parameters.

Upon estimating the parameter from the scale-invariant spectra, the interesting result is that the vector mode creates the B-mode polarization without modifying the large-scale temperature spectrum, compared with the tensor mode. When varying the spectral indices, in which the tensor power spectrum may be tilted, the tensor mode with a large blue tilt fits both the *Planck* and the BICEP2 data. This is because the large-scale temperature spectrum induced by the tensor mode can be suppressed and the tensor mode does not destroy the scalar mode fit to the large scale temperature data from *Planck*. In this case, we should note that the large-scale B-mode polarization is also suppressed and the bump from the reionization epoch vanishes. Thus, a precise observation of the reionization bump is important. The best chance upcoming experiments will have of revealing the source of the B-mode polarization spectrum is by observing the spectrum on large scales, as experiments aiming at smaller scales must differentiate between the primordial signal and the lensing B-mode contaminant. Precise observations at large scales could clarify the source of the primordial B-mode spectrum: blue tensor modes, "standard" tensor modes or vector modes.

The vector mode can also produce magnetic fields in the primordial photon and baryon plasma. The parameter values allowed by the *Planck* and BICEP2 data set indicate that the strength of the resulting magnetic fields is about 10^{-22} Gauss at $k = 0.1$ Mpc^{-1} at cosmological recombination. This value is comparable to or slightly less than that needed to explain the observed large-scale magnetic fields; namely, $\mathcal{O}(10^{-21})$ Gauss.

The current CMB data are well described by the existence of slightly red primordial vector mode, which may play a role in generating cosmic magnetic fields. Probing early-Universe models that produce such vector modes is an exciting avenue for future research.

Acknowledgments

This work was supported in part by a Grant-in-Aid for JSPS Research under Grants Nos. 26-63 (SS) and 25-573 (MS), and a Grant-in-Aid for Scientific Research under No. 24340048 (KI). M.S. was also supported in part by the ASI/INAF Agreement I/072/09/0 for the Planck LFI Activity of Phase E2. We also acknowledge the Kobayashi-Maskawa Institute for the Origin of Particles and the Universe, Nagoya University, for providing computing resources useful in conducting the research reported in this paper. This research has also been supported in part by World Premier International Research Center Initiative, the Ministry of Education, Culture, Sports, Science and Technology, Japan.

References

[1] U. Seljak and A. Slosar, *B polarization of cosmic microwave background as a tracer of strings*, *Phys.Rev.* **D74** (2006) 063523, [astro-ph/0604143].

[2] A. Lewis, *CMB anisotropies from primordial inhomogeneous magnetic fields*, *Phys.Rev.* **D70** (2004) 043011, [astro-ph/0406096].

[3] T. Jacobson and D. Mattingly, *Gravity with a dynamical preferred frame*, *Phys.Rev.* **D64** (2001) 024028, [gr-qc/0007031].

[4] C. Bennett, A. Banday, K. Gorski, G. Hinshaw, P. Jackson, et al., *Four year COBE DMR cosmic microwave background observations: Maps and basic results*, *Astrophys.J.* **464** (1996) L1–L4, [astro-ph/9601067].

[5] **WMAP** Collaboration, C. Bennett et al., *Nine-Year Wilkinson Microwave Anisotropy Probe (WMAP) Observations: Final Maps and Results*, *Astrophys.J.Suppl.* **208** (2013) 20, [arXiv:1212.5225].

[6] **Planck Collaboration** Collaboration, P. Ade et al., *Planck 2013 results. I. Overview of products and scientific results*, arXiv:1303.5062.

[7] **Planck Collaboration** Collaboration, P. Ade et al., *Planck 2013 results. XVI. Cosmological parameters*, arXiv:1303.5076.

[8] M. Kamionkowski, A. Kosowsky, and A. Stebbins, *A Probe of primordial gravity waves and vorticity*, *Phys.Rev.Lett.* **78** (1997) 2058–2061, [astro-ph/9609132].

[9] U. Seljak and M. Zaldarriaga, *Signature of gravity waves in polarization of the microwave background*, *Phys.Rev.Lett.* **78** (1997) 2054–2057, [astro-ph/9609169].

[10] M. Zaldarriaga and U. Seljak, *An all sky analysis of polarization in the microwave background*, *Phys.Rev.* **D55** (1997) 1830–1840, [astro-ph/9609170].

[11] **BICEP2 Collaboration** Collaboration, P. Ade et al., *Detection of B-Mode Polarization at Degree Angular Scales by BICEP2*, *Phys.Rev.Lett.* **112** (2014) 241101, [arXiv:1403.3985].

[12] A. A. Starobinskiĭ, *Spectrum of relict gravitational radiation and the early state of the universe*, *Soviet Journal of Experimental and Theoretical Physics Letters* **30** (Dec., 1979) 682.

[13] V. A. Rubakov, M. V. Sazhin, and A. V. Veryaskin, *Graviton creation in the inflationary universe and the grand unification scale*, *Physics Letters B* **115** (Sept., 1982) 189–192.

[14] J. R. Pritchard and M. Kamionkowski, *Cosmic microwave background fluctuations from gravitational waves: An Analytic approach*, *Annals Phys.* **318** (2005) 2–36, [astro-ph/0412581].

[15] M. Kawasaki and S. Yokoyama, *Compensation for large tensor modes with iso-curvature perturbations in CMB anisotropies*, *ArXiv e-prints* (Mar., 2014) [arXiv:1403.5823].

[16] C. R. Contaldi, M. Peloso, and L. Sorbo, *Suppressing the impact of a high tensor-to-scalar ratio on the temperature anisotropies*, arXiv:1403.4596.

[17] M. Kawasaki, T. Sekiguchi, T. Takahashi, and S. Yokoyama, *Isocurvature perturbations and tensor mode in light of Planck and BICEP2*, arXiv:1404.2175.

[18] A. Moss and L. Pogosian, *Did BICEP2 see vector modes? First B-mode constraints on cosmic defects*, arXiv:1403.6105.

[19] J. Lizarraga, J. Urrestilla, D. Daverio, M. Hindmarsh, M. Kunz, et al., *Can topological defects mimic the BICEP2 B-mode signal?*, arXiv:1403.4924.

[20] C. Bonvin, R. Durrer, and R. Maartens, *Can primordial magnetic fields be the origin of the BICEP2 data?*, *ArXiv e-prints* (Mar., 2014) [arXiv:1403.6768].

[21] R. Durrer, D. G. Figueroa, and M. Kunz, *Can Self-Ordering Scalar Fields explain the BICEP2 B-mode signal?*, arXiv:1404.3855.

[22] M. J. Mortonson and U. Seljak, *A joint analysis of Planck and BICEP2 B modes including dust polarization uncertainty*, arXiv:1405.5857.

[23] K. Ichiki, K. Takahashi, and N. Sugiyama, *Constraint on the primordial vector mode and its magnetic field generation from seven-year Wilkinson Microwave Anisotropy Probe Observations*, *Phys.Rev.* **D85** (2012) 043009, [arXiv:1112.4705].

[24] A. Rebhan, *Large-scale rotational perturbations of a Friedmann universe with collisionless matter and primordial magnetic fields*, *Astrophys.J.* **392** (June, 1992) 385–393.

[25] A. Lewis, *Observable primordial vector modes*, *Phys.Rev.* **D70** (2004) 043518, [astro-ph/0403583].

[26] F. Beutler, C. Blake, M. Colless, D. H. Jones, L. Staveley-Smith, L. Campbell, Q. Parker, W. Saunders, and F. Watson, *The 6dF Galaxy Survey: baryon acoustic oscillations and the local Hubble constant*, MNRAS **416** (Oct., 2011) 3017–3032, [arXiv:1106.3366].

[27] N. Padmanabhan, X. Xu, D. J. Eisenstein, R. Scalzo, A. J. Cuesta, K. T. Mehta, and E. Kazin, *A 2 per cent distance to $z = 0.35$ by reconstructing baryon acoustic oscillations - I. Methods and application to the Sloan Digital Sky Survey*, MNRAS **427** (Dec., 2012) 2132–2145, [arXiv:1202.0090].

[28] L. Anderson, E. Aubourg, S. Bailey, D. Bizyaev, M. Blanton, A. S. Bolton, J. Brinkmann, J. R. Brownstein, A. Burden, A. J. Cuesta, L. A. N. da Costa, K. S. Dawson, R. de Putter, D. J. Eisenstein, J. E. Gunn, H. Guo, J.-C. Hamilton, P. Harding, S. Ho, K. Honscheid, E. Kazin, D. Kirkby, J.-P. Kneib, A. Labatie, C. Loomis, R. H. Lupton, E. Malanushenko, V. Malanushenko, R. Mandelbaum, M. Manera, C. Maraston, C. K. McBride, K. T. Mehta, O. Mena, F. Montesano, D. Muna, R. C. Nichol, S. E. Nuza, M. D. Olmstead, D. Oravetz, N. Padmanabhan, N. Palanque-Delabrouille, K. Pan, J. Parejko, I. Pâris, W. J. Percival, P. Petitjean, F. Prada, B. Reid, N. A. Roe, A. J. Ross, N. P. Ross, L. Samushia, A. G. Sánchez, D. J. Schlegel, D. P. Schneider, C. G. Scóccola, H.-J. Seo, E. S. Sheldon, A. Simmons, R. A. Skibba, M. A. Strauss, M. E. C. Swanson, D. Thomas, J. L. Tinker, R. Tojeiro, M. V. Magaña, L. Verde, C. Wagner, D. A. Wake, B. A. Weaver, D. H. Weinberg, M. White, X. Xu, C. Yèche, I. Zehavi, and G.-B. Zhao, *The clustering of galaxies in the SDSS-III Baryon Oscillation Spectroscopic Survey: baryon acoustic oscillations in the Data Release 9 spectroscopic galaxy sample*, MNRAS **427** (Dec., 2012) 3435–3467, [arXiv:1203.6594].

[29] A. Lewis and S. Bridle, *Cosmological parameters from CMB and other data: A Monte Carlo approach*, *Phys.Rev.* **D66** (2002) 103511, [astro-ph/0205436].

[30] Y. Wang and W. Xue, *Inflation and Alternatives with Blue Tensor Spectra*, arXiv:1403.5817.

[31] M. Gerbino, A. Marchini, L. Pagano, L. Salvati, E. Di Valentino, et al., *Blue Gravity Waves from BICEP2 ?*, arXiv:1403.5732.

[32] Z.-G. Liu, H. Li, and Y.-S. Piao, *Pre-inflationary genesis with CMB B-mode polarization*, arXiv:1405.1188.

[33] **The POLARBEAR Collaboration** Collaboration, P. Ade et al., *A Measurement of the Cosmic Microwave Background B-Mode Polarization Power Spectrum at Sub-Degree Scales with POLARBEAR*, arXiv:1403.2369.

[34] L. M. Widrow, D. Ryu, D. R. Schleicher, K. Subramanian, C. G. Tsagas, et al., *The First Magnetic Fields*, *Space Sci.Rev.* **166** (2012) 37–70, [arXiv:1109.4052].

[35] A.-C. Davis, M. Lilley, and O. Tornkvist, *Relaxing the bounds on primordial magnetic seed fields*, *Phys.Rev.* **D60** (1999) 021301, [astro-ph/9904022].